# Analysis of the drought recovery of Andosols on southern Ecuadorian Andean páramos

**V. Iñiguez [1, 2, 3], O. Morales[1], F. Cisneros[1], W. Bauwens[2], G. Wyseure[3]**

[1]{Programa para el manejo del Agua y del Suelo (PROMAS), Universidad de Cuenca, Cuenca, Ecuador}

[2]{Department of Hydrology and Hydraulic Engineering, Earth System Sciences Group, Vrije Universiteit Brussel (VUB), Brussels, Belgium}

[3]{Department of Earth and Environmental Science, KU Leuven, Leuven, Belgium}

Correspondence to: vicente.iniguez@ucuenca.edu.ec

## Abstract

The Neotropical Andean grasslands above 3500 m a.s.l., known as páramo, offer remarkable ecological services for the Andean region. The most important of these is the water supply of excellent quality to many cities and villages in the inter-Andean valleys and along the coast. The páramo ecosystem and especially its soils are under constant and increased threat by human activities and climate change. In this study, the recovery speed of the páramo soils after drought periods are analysed. The observation period includes the droughts of 2009, 2010, 2011 and 2012 together with intermediate wet periods. Two experimental catchments – one with and one without páramo– were investigated. The Probability Distributed Moisture (PDM) model was calibrated and validated in both catchments. Drought periods and its characteristics were identified and quantified by a threshold level approach and complemented by means of a drought propagation analysis. At the plot scale in the páramo region, the soil water content measured by TDR probes dropped from a normal value of about 0.84 to ~ 0.60 $cm^3$ $cm^{-3}$, while the recovery time was two to three months. This did not occur at lower altitudes (Cumbe) where the soils are mineral. Although the soil moisture depletion observed in these soils was similar to that of the Andosols (27%), decreasing from a normal value of about 0.54 to ~ 0.39 $cm^3$ $cm^{-3}$, the recovery was much slower and took about eight months for the drought in 2010. At the catchment scale, however, the soil water storage simulated by the PDM model and the drought analysis was not as pronounced. Soil moisture

droughts occurred mainly in the dry season in both catchments. The deficit for all cases is small and progressively reduced during the wet season. Vegetation stress periods correspond mainly to the months of September, October and November, which coincides with the dry season. The maximum number of consecutive dry days were reached during the drought of 2009 and 2010 (19 and 22 days), which can be considered to be a long period in the páramo. The main factor in the hydrological response of these experimental catchments is the precipitation relative to the potential evapotranspiration. As the soils never became extremely dry nor close to the wilting point, the soil water storage capacity had a secondary influence.

## 1 Introduction

In the northern Andean landscape, between ca. 3500 and 4500 m a.s.l., an "alpine" Neotropical grassland ecosystem -locally known as "páramo"- covers the mountains. The major ecological characteristics of this ecosystem have been documented by several authors (e.g. Buytaert et al., 2006a; Hofstede et al., 2003; Luteyn, 1999). The páramo is an endemic ecosystem with high biodiversity. Its soils contain an important carbon storage and provide a constant source of drinking water for many cities, villages, irrigation systems and hydro-power plants. During recent years, a high vulnerability to changes induced by human activities and climate change in mountainous regions has been recognized in these systems. Most of the research in páramos has been focused on its hydrological capacity as well as the soil characteristics under unaltered and altered conditions (Buytaert et al., 2007a; Farley et al., 2004; Hofstede et al., 2002; Podwojewski et al., 2002). These research projects recognize the key role of the páramos in the water supply in the Andean region. The hydrological capacity is mainly related to the characteristics of its soils. Shallow organic soils classified according to the World Reference Base for Soil Resources (WRB) as Andosols and Histosols (FAO et al., 1998) are the two main groups of soils that can be found in this Andean region. In addition, but less frequently, also Umbrisols, Regosols and other soils may be found. These soils are characterized by high levels of organic matter. They have an immense water storage capacity which reduces flood hazards for the downstream areas, while sustaining the low flows all year round for domestic, industrial and environmental uses.

In the wet páramos that we investigated –and which have a low seasonal climate variability– the high water production can be explained by the combination of a somewhat higher precipitation and -more importantly- a lower water consumption by the vegetation. In these

conditions, the role of the soil water storage capacity would not be significant. This is in contrast with páramos with a more distinct seasonal rainfall variability (e.g., in the western part of the highlands of the Paute river basin), where the hydrological behaviour of the páramo ecosystem is more influenced by the water holding capacity of the soils (Buytaert et al., 2006a). Rainfall ranges between 1000 and 1500 mm $year^{-1}$ and is characterized by frequent, low volume events (drizzle) (Buytaert et al., 2007b). The annual runoff can be as high as 67% of the annual rainfall (Buytaert et al., 2006a). During wet periods the volumetric soil water content ranges between 80% and 90%, with a wilting point of around 40%. Therefore, the soil water holding capacity is high as compared to mineral soils. This is a very important factor in the hydrological behaviour of the páramo. This larger storage is important during dry periods and explains the sustained base flow throughout the year. The physical characteristics of the soil such as porosity and microporosity –which are much higher than that commonly found in most soil types– explains an important part of the regulation capacity during dry periods. The water buffering capacity of these ecosystems can also be explained by the topography, as the irregular landscape contains many concavities and local depressions where bogs and small lakes have developed (Buytaert et al., 2006a).

Nevertheless, the páramo area is under threat by the advance of the agricultural frontier. Additionally, flawed agricultural practices cause soil degradation and erosion. Former studies on soil water erosion reveal significant soil loss in the highlands of the Ecuadorian Andean as result of land use changes (Vanacker et al., 2007), but also tillage erosion is responsible for this soil loss and for the degradation of the water holding capacity (Buytaert et al., 2005; Dercon et al., 2007).

Land cover changes also occurred in the páramo. In the seventies, some areas of páramo were considered appropriate for afforestation with exotic species such as *Pinus radiate* and *Pinus patula*. The main goal was to obtain an economical benefit from this commercial timber. The negative impact of this afforestation and the consequences on the water yield of the páramo have been described by Buytaert et al. (2007b). In addition, the productivity was often rather disappointing, due to the altitude.

The potential impact of the climate change over alpine ecosystems has also been reported by Buytaert et al., 2011and Viviroli et al., 2011. Mora et al. (2014) predicted an increase in the mean annual precipitation and temperature in the region that is of interest to our study. Therefore, the carbon storage and the water yield could be reduced by the higher temperatures

and the larger climate variability. However, the uncertainties of the potential impact of the climate change remain high (Buytaert and De Bièvre, 2012; Buytaert et al., 2010).

Additionally, the occurrence of drought periods in the páramo has a negative impact on the water supply and on the economy of the whole region that depends on water supply from the Andes. For instance, the water levels in the reservoir of the main hydropower project in the Ecuadorian Andes –the Paute Molino project– reached their lowest values as a consequence of the drought between December 2009 and February 2010. This caused several, intermittent, power cuts in many regions of Ecuador. The power plant's capacity is 1075 MW. In that period the Paute Molino hydropower provided around 60% of Ecuador's electricity (Southgate and Macke, 1989).

It is claimed that the hydrological regulation and buffering capacity is linked to its soils (Buytaert et al., 2007b). Therefore, the present study investigated the response of páramo soils to drought and compared it with other soils on grasslands at lower altitude in the same region. The drought analysed was a hydrological and soil water drought as defined by Van Loon (2015).

The major objective of our research was to analyse the recovery speed of the páramo soils after drought periods. Indeed, our hydrological perspective serves -in the first place- the downstream users. The observation period included the droughts of 2009, 2010, 2011 and 2012 together with intermediate wet periods.

In this paper hydrological drought was compared and related to soil water drought by analysing the drought propagation. Two experimental catchments –one with and one without páramo– were investigated. The results from the hydrological model and drought analysis in terms of soil water storage were compared. In the two catchments: rainfall, climate, flow and soil moisture by TDR in experimental plots were measured. A parsimonious conceptual hydrological model –the Probability Distributed Moisture simulator (PDM)– was calibrated and validated for each experimental catchment. The PDM model allowed us to analyse the temporal and spatial variability of the soil water content as well as the maximum storage capacity at the catchment scale.

In this context, the hydrological model (PDM) used in the research tried to link soil moisture storage (as an indicator for soil water drought) with the stream discharge (as an indicator for the hydrological drought).

## 2 Materials

### 2.1 The study area

The catchments under study are located in the southwest highlands of the Paute river basin, which drains to the Amazon River (Fig. 1). These highlands form part of the Western Cordillera in the Ecuadorian Andes with a maximum altitude of 4420 m a.s.l. The study area comprises of a mountain range from 2647 to 3882 m a.s.l. Two catchments have been selected from this region: Calluancay and Cumbe.

The Calluancay catchment has an area of 4.39 $km^2$ with an altitude range between 3589 and 3882 m a.s.l. and a homogeneous páramo cover. The páramo vegetation consists mainly of tussock or bunch grasses and very few trees of the genus *Polylepis*. These trees are observed in patches sheltered from the strong winds by rock cliffs or along to some river banks in the valleys. Furthermore, in saturated areas or wetlands huge cushion plants are surrounded by mosses. This vegetation is adapted to extreme weather conditions such as low temperatures at night, intense ultra-violet radiation, the drying effect of strong winds and frequent fires (Luteyn, 1999). The land use of Calluancay is characterized by extensive livestock grazing.

The second catchment, Cumbe, drains an area of 44 $km^2$. The highest altitude reaches 3467 m a.s.l., whereas the outlet is at an altitude of 2647 m. This altitude range of almost 1000 m defines a typical Andean mountain landscape with steep slopes and narrow valleys where the human intervention is also evident. This catchment is below 3500 m and therefore, contains a negligible area of páramo. The most prominent land cover is grassland (38.1%) along with arable land and rural residential areas (26.9%). A sharp division between the residential areas and the small scale fields is absent. Mountain forest remnants are scattered and cover 23% of the area, often on the steeper slopes. At the highest altitude (>3300 m) sub-páramo is predominant; it occupies only 7.6% of the catchment. In the Cumbe catchment, about 4.4% of the area is degraded by landslides and erosion.

A small village, “Cumbe”, is located in the valley and at the lower altitudes of the catchment. This village has ca. 5550 inhabitants. The water diversions from streams in Cumbe amount to ca. 12 l/s, mainly for drinking water. Additionally, during dry periods two main open water channels for surface irrigation are enabled. The water diversion and its rudimentary hydraulic structures have been built upstream of the outlet of the catchment. These irrigation systems deliver water to the valley area occupied by grasslands and small fields with crops.

Several types of soils can be identified in Cumbe and Calluancay, which are mainly conditioned by the topography. Dercon et al. (1998, 2007) have described the more common toposequences in the southern Ecuadorian Andes according to the WRB classification (FAO et al., 1998). Cumbe has a toposequence of soils from Vertic Cambisols, located in the alluvial area, surrounded by Dystric Cambisols at the hillslopes in the lower and middle part of the catchment. Eutric Cambisols or Humic Umbrisols extend underneath the forest patches between 3000 and 3300 m a.s.l. The highest part of the catchment -from 3330 to 3467 m a.s.l.- is covered by Humic Umbrisols or Andosols.

In contrast, Calluancay is characterized by two groups of organic soils under páramo: Andosols (in the higher and steeper parts) and Histosols (in the lower and gentler parts of the catchment). The soils were formed from igneous rocks, such as andesitic lava and pyroclastic igneous rock (mainly the Quimsacocha and Tarqui formations, dating from the Miocene and Pleistocene respectively), forming an impermeable bedrock underneath the catchment. In the Cumbe catchment, the highlands and some areas of the middle part (about 55% of the area) are characterized by pyroclastic igneous rocks (mainly the Tarqui formation). The valley area (37% of the basin) is covered by sedimentary rocks like mudstones and sandstones (mainly the Yunguilla formation, dating from the upper Cretaceous). Only 8% of the Cumbe catchment comprises alluvial and colluvial deposits, which date from the Holocene (Hungerbühler et al., 2002).

## 2.2 Monitoring of hydro-meteorological data

An intensive monitoring with a high time resolution was carried out in the study area over a period of 28 months.

The gauging station at the outlet of Cumbe consists of a concrete trapezoidal supercritical-flow flume (Kilpatrick and Schneider, 1983) and a water level sensor (WL16 - Global Water). Data logging occurs at a 15 minute time interval. Regular field measurements of the discharge were carried out to cross-check the rating curve. Initially a smaller catchment, similar in size to Calluancay, was also equipped within the Cumbe catchment but a landslide destroyed and covered this flume. Hence, unfortunately no data was collected.

The measurements at Calluancay were part of a larger hydrological monitoring network maintained by PROMAS. Water levels were logged every 15 minutes at two gauging stations, which consist of a concrete V-shaped weir with sharp metal edges and a water level sensor

(WL16- Global Water). The first station was installed at the outlet of the catchment. The second gauging station monitors an irrigation canal to which water is diverted from the main river. The gauging station was installed where the canal passes the water divide of the catchment. Therefore, the total discharge can be evaluated.

For Calluancay, rainfall is measured by a tipping bucket rain gauge (RG3M-Onset HOBO Data Loggers) located inside the catchment and with a resolution of 0.2 mm.

Three similar rain gauges were installed in the larger Cumbe catchment and located at the high, middle and lower part of the catchment. The areal rainfall for Cumbe was calculated with the inverse distance weighing (IDW) method, using the R implementation of GSTAT (Pebesma, 2004).

In each experimental catchment the meteorological variables, such as: air temperature, relative humidity, solar radiation and wind speed, were measured with a 15 minute time interval by an automatic weather station. These stations were used to estimate the potential reference evapotranspiration according to the FAO-Penman-Monteith equation.

### 2.3 The measurement of the soil water content

In both catchments, the soil moisture content of the top soil layer was measured by means of time domain reflectometry (TDR) probes at representative sites in the vicinity of the weather stations. In each catchment there was one plot equipped with 6 TDRs with a data-logger.

As TDR-sensors with data-logger per plot require a large investment, the locations for the TDR measurements were carefully selected based on a digital terrain analysis, the soil and land cover maps and field surveys (soil profile pits). In Calluancay, the soil information was available from former studies by PROMAS between 2007 and 2009. In this period, a soil map (scale 1:10 000) -which covered the whole altitudinal range of the páramo (3500-3882 m a.s.l.)- was generated based on soil descriptions of 2095 vertical boreholes and 12 soil profile pits. For each soil profile pit a physico-chemical analysis of each layer was executed. Within the Cumbe catchment, 13 soil profile pits were dug as part of the present research. Thus, for both catchments a detailed soil map was available covering the whole altitudinal range (2647 – 3882 m a.s.l.). Based on this detailed soil information representative locations for the TDR measurements in each catchment were selected.

The TDRs were installed vertically from the soil surface with a length of 30 cm and logged at 15 minute time intervals. In Calluancay, every fortnight soil water content was also measured by sampling from November 2007 until November 2008. In this catchment the TDR time series was from May 2009 until November 2012. In Cumbe, the TDR-time series extended from July 2010 until November 2012.

For Cumbe and Calluancay, the TDR probes were calibrated based on gravimetric measurements of soil moisture content, using undisturbed soil samples ($r^2$ = 0.79 and 0.80 respectively). In addition, the curves were regularly cross-validated by undisturbed soil samples during the monitoring period.

The soil water retention curves were determined based on undisturbed and disturbed soil samples collected near to the TDR probes. In the laboratory, pressure chambers in combination with a multi-step approach allowed us to define pairs of values for moisture ($\theta$) and matric potential (h). The soil water retention curve model proposed by van Genuchten (1980) was fitted on the data.

# 3 Methods

## 3.1 The catchment modelling

The hydrological PDM model (Moore and Clarke, 1981; Moore, 1985) is a conceptual rainfall – runoff model, which consists of two modules. The first one is the soil moisture accounting (SMA) module which is based on a distribution of soil moisture storages with different capacities accounting for the spatial heterogeneity in a catchment. The probability distribution used is the Pareto distribution. The SMA module simulates the temporal variation of the average soil water storage. The second part of the model structure is the routing module, which consists of two linear reservoirs in parallel, in order to model the fast and slow flow pathways, respectively.

Based on geological data, the deep percolation and the capillary rise fluxes in Calluancay are considered to be negligible since the soils overlay bedrock consisting of igneous rocks with limited permeability. In the páramos, saturation overland flow is the dominant flow process of fast runoff generation (Buytaert and Beven, 2011). Lateral subsurface flow has a slower response. Therefore, the stream discharge at the outlet of the catchment thus comprises mainly of fast overland flow and slow lateral flow.

In Cumbe, a surface-based electrical resistivity tomography test (Koch et al., 2009; Romano, 2014; Schneider et al., 2011) of a cross-section revealed no significant shallow groundwater for the alluvial area. In addition, the flat alluvial area surrounding the river near the catchment outlet is very small (2.7 % of the catchment area). Therefore, deep percolation and capillary rise are also regarded to be negligible.

As clay is the most important soil texture in Cumbe it is inferred that the infiltration overland flow is the dominant flow process of runoff generation. As a result, the stream discharge in Cumbe consists, as in Calluancay, of the combination of overland flow due to either limited infiltration or saturation and of shallow lateral flow.

The PDM model was implemented within a MATLAB toolbox using the options of calculating the actual evapotranspiration $E_a$ as a function of the potential evaporation rate $E_p$ and the soil moisture deficit by (Wagener et al., 2001):

$$E_a = \left\{1 - \left[\frac{\left(S_{max} - S(t)\right)}{S_{max}}\right]\right\} \cdot E_p \quad (1)$$

Where, $S_{max}$ is the maximum storage and $S(t)$ is the actual storage at the beginning of the interval. A description of the model parameters is provided in Table 2.

The actual evapotranspiration estimated by the PDM model as compared to the potential vegetation evapotranspiration is an indicator of the drought stress.

### 3.1.1 The potential evapotranspiration

The FAO-Penman-Monteith approach (Allen et al., 1998) was used to estimate the potential evapotranspiration of a reference crop (similar to short grass) under stress free conditions without water limitation:

$$E_p = \frac{0.408\Delta(R_n - G_h) + \gamma \frac{900}{T + 273} u_2 (e_s - e_a)}{\Delta + \gamma(1 + 0.34u_2)} \quad (2)$$

Where:

$E_p$ = the potential reference evapotranspiration [mm day$^{-1}$],

$R_n$ = the net radiation at the crop surface [MJ m$^{-2}$ day$^{-1}$],

$G_h$ = the soil heat flux density [MJ m$^{-2}$ day$^{-1}$],

$T$ = the mean daily air temperature at 2 m height [$^o$C],

$u_2$ = the wind speed at 2 m height [m s$^{-1}$],

$e_s$ = the saturation vapour pressure [kPa],

$e_a$ = the actual vapour pressure [kPa],

$e_s - e_a$ = the saturation vapour pressure deficit [kPa],

$\Delta$ = the slope of the vapour pressure curve [kPa $^o$C$^{-1}$],

$\gamma$ = the psychrometric constant [kPa $^o$C$^{-1}$].

The suitability of the FAO-Penman-Monteith approach for high altitudinal areas has been evaluated by Garcia et al. (2004). They found that the FAO-approach gives the smallest bias (-0.2 mm day$^{-1}$) as compared to lysimetric measurements.

The measurements of the solar radiation by the meteorological stations in our experimental catchments were not consistent and considered to be unreliable. Therefore, the solar radiation was estimated by the Hargreaves-Samani equation (Hargreaves and Samani, 1985) using the daily maximum and minimum air temperature:

$$R_s = R_a \, c \, (T_{max} - T_{min})^{0.5} \quad (3)$$

Where:

$R_s$ = the solar radiation [MJ m$^{-2}$ day$^{-1}$],

$R_a$ = the extra-terrestrial solar radiation [MJ m$^{-2}$ day$^{-1}$],

$c$ = an empirical coefficient [-],

$T_{max}$, $T_{min}$ = the daily maximum and minimum air temperature respectively [$^o$C],

According to Hargreaves and Samani (1985) "*c*" has a value of 0.17 for inland areas.

### 3.1.2 The actual evapotranspiration

The potential evapotranspiration of vegetation without drought stress can be calculated by multiplying the reference crop evapotranspiration by vegetation coefficient $k_v$. During dry periods, with water stress, the vegetation extracts less water as compared to the vegetation requirement. Due to this, the relative reduction of the evapotranspiration may be expressed by a water stress coefficient $k_s$. During stress free periods $k_s$ equals to one and the lower the stress coefficient the more stress the vegetation experiences.

The actual evapotranspiration, $E_a$, can thus be calculated as:

$$E_a = k_s \cdot k_v \cdot E_p \quad (4)$$

In general, $k_v$ is time-dependent, as it is linked to the growth cycle of the vegetation and thus to the season. For páramo close to the equator, this seasonality may be neglected as the grasses are slow-growing and perennial.

For the purpose of this study the global effect of the two coefficients will be estimated and the Eq. (4) can be combined into one coefficient *K*:

$$E_a = K \cdot E_p \quad (5)$$

In order to determine *K* the actual and potential evapotranspiration need to be estimated.

### 3.1.3 Calibration and validation of the PDM model

A split sample test was performed in order to assess the performance of the PDM model and so, calibration and validation periods were established (Klemeš, 1986). The collected data contained wet and dry periods.

To implement the PDM model, an exploratory sensitivity analysis was done in order to define the feasible parameter range. The sampling strategy applied was an optimal Latin Hypercube sampling with a genetic algorithm according to (Stocki, 2005) and (Liefvendahl and Stocki, 2006). Afterwards, the parameters of the PDM model were optimized by means of the Shuffled Complex Evolution algorithm (Duan et al., 1992).

The time periods from 29 November 2007 until 06 August 2009 and from 20 May 2010 until 27 November 2012 were used as calibration and validation periods respectively for Calluancay. In the case of Cumbe, the calibration and validation periods were respectively from 21 April 2009 until 17 April 2011 and from 18 April 2011 until 13 December 2012. The selected periods for calibration and validation contained the typical climatic conditions of the southern Ecuadorian Andes (Buytaert et al., 2006b; Celleri et al., 2007).

The Nash and Sutcliffe efficiency (NSE) was used as objective function (Nash and Sutcliffe, 1970) for calibration. As low flows under drought were important the logarithmic discharges were used for the calculation of the NSE.

It is important to mention that the measured soil moisture data were not used as input variables to the model. However, as most hydrological models the PDM model generates internally state and output variables. These internally calculated variables include: effective rainfall, actual evapotranspiration, simulated discharge and average distribution characteristics of the soil moisture storage. After calibration/validation of the parameters, however, the simulated PDM average soil water content was compared to the observed soil water content, measured by TDR in one experimental plot in each catchment. The average soil water content simulated by PDM was used in the drought analysis.

PDM does not explicitly model the soil surface evaporation. Consequently, it cannot estimate the soil water storage below the wilting point. The soil water content thus always remained higher than wilting point. The volumetric water storage at wilting point, which is still as high as 40% in Andosols and Histosols, was therefore not actively represented in the model and can be considered as dead storage from the PDM modelling point of view.

### 3.2 The drought analysis

The severity of drought periods was identified and quantified by a threshold level approach (Andreadis et al., 2005; Van Lanen et al., 2013; Van Loon et al., 2014). Thresholds were set

for the time series of precipitation ($P$), observed stream discharge ($Q$) and average soil water content simulated by PDM ($S$), according to Van Loon et al. (2014):

- A threshold for each month of the year was based on the 80$^{th}$ percentile of the duration curves of $P$, $S$ and $Q$, applying a 10 day moving average. This threshold was subsequently smoothed by a 30 day moving average. A last smoothing removed the stepwise pattern and avoided artefact droughts at the beginning or end of a month (Van Loon, 2013).

- Drought characteristics are determined based on a deficit index:

$$d(t) = \begin{cases} \tau(t) - x(t) & if\ x(t) < \tau(t) \\ & or \\ 0 & if\ x(t) \geq \tau(t) \end{cases} \quad (6)$$

where, $x(t)$ is the hydro-meteorological variable on time $t$ and $\tau(t)$ is the threshold level of the hydrological variable. The units are mm day$^{-1}$ and the time is measured in days. The deficit of a drought event $i$ ($D_i$) is then given by

$$D_i = \sum_{t=1}^{T} d(t) \,.\, \Delta t \quad (7)$$

in which $D_i$ is in mm. The deficit is standardized by dividing $D_i$ by the mean of the hydro-meteorological variable $x(t)$. A physical interpretation of the standardized deficit is the number of days with mean flow that is required to reduce the deficit to zero (Van Loon et al., 2014).

### 3.2.1 Drought propagation and drought recovery analysis

Here, we analysed the translation -as a chain of hydrological processes- from meteorological drought over soil water drought into hydrological drought for the catchment. The time series of $P$, $Q$ and $S$ were plotted on the same figure per catchment. This allowed a visual inspection

of the propagation, onset and recovery of droughts and a comparison of the behaviour of the different time series.

Fig. 2 shows a conceptual graph for the estimation of the drought recovery. This diagram is similar to that presented by Parry et al. (2016), who have proposed an approach for the systematic assessment of the drought recovery period or drought termination. Such graphs allow us to determine the duration $t_d$ of a drought. The drought starts when the variable drops under the threshold and ends when the normal state is reached again. To estimate the duration of the drought recovery, $t_{dr}$, it is assumed that the recovery starts from the lowest value of the variable and ends at the end of the drought. The slope of the variable between the lowest point and the end estimates the rate of recovery. This rate can be expressed as a percentage of the recovery per day with respect to the normal value of the variable.

### 3.2.2 Vegetation stress and recovery

Drought indices have been used by several researchers in order to quantify drought characteristics (Dai, 2011; Van Loon, 2015; Tsakiris et al., 2013). Most of them are based on precipitation (*P)* and potential evapotranspiration ($E_p$). For instance, the Standardized Precipitation Index (SPI) (Lloyd-Hughes and Saunders, 2002) or the Standardized Precipitation and Evapotranspiration Index (SPEI) (Vicente-Serrano et al., 2013) are widely used in drought studies. Due to the lack of a long historical time series of climate data for our experimental area, however, this type of indices cannot be applied. Nevertheless, based on the available monthly time series of $P$ and $E_p$ a comparison can be made between catchments.

For this purpose, vegetation stress is assumed to occur when the monthly potential evapotranspiration exceeds the monthly rainfall:

$$E_p > P \tag{8}$$

Similarly, the duration of a stress period is defined as the sum of consecutive months where vegetation stress is identified. Modelling by PDM was used to estimate $E_a$ and was compared with the $E_p$.

After a stress period, when the wet season starts, $P$ reaches values that allow to cover the deficit of the soil water and the vegetation starts to recover. These periods are also identified based on the monthly data of $P$ and $E_p$ and contrasted with $E_a$ estimations. When $E_a$ reaches

the highest value -normally during the wet season- that month marks the end of the vegetation recovery.

### 3.2.3 The sensitivity analysis

A sensitivity analysis was carried out with the PDM model in order to reveal the most important factor in the recovery of the soils after drought periods. The considered factors relate to climate -precipitation and potential evapotranspiration- and to soil characteristics.

The parameters set obtained during the calibration procedure -which closely resemble the soil water storage characteristics for each catchment- is the first factor *S*. The second and third factors are precipitation *P* and potential evapotranspiration $E_p$. Two scenarios were regarded: 1) For Calluancay, the parameters which defined the *S* were not modified in the model but *P* and $E_p$ based on meteorological data in Cumbe were used as input data in order to assess the impact on *S*. The same scenario was applied to Cumbe, the *S* defined by the parameters set calibrated were not modified but *P* and $E_p$ registered in Calluancay were regarded as input data to the model of Cumbe.

2) The *S* and *P* in both catchments were not modified but the $E_p$ was exchanged.

The scenario results, simulated stream discharge $Q_{sim}$ and average soil water storage *S* are displayed in plots for each catchment in order to establish the main differences. Positive or negative deviations from the original simulation (calibration) will reveal the impact of the climate over the soil water storage and stream discharge. The analysis of the scenario results is focused on the drought recovery periods in order to compare the behaviour of the soils during different climate conditions.

## 4 Results and discussion

### 4.1 Potential evapotranspiration

The potential reference evapotranspiration ($E_p$) for the period from 16 July 2010 until 15 November 2012 was calculated by the FAO-Penman-Monteith approach with the solar radiation estimated by Hargreaves-Samani. The daily average of $E_p$ for Calluancay and Cumbe was 2.35 and 3.04 mm $day^{-1}$ respectively. The temporal variation of $E_p$ is depicted in

Fig. 3. It reveals a sinusoidal pattern with higher atmospheric evaporative demand during the drier months (from August to March) and a lesser demand during the subsequent wet periods (from April to July). $E_p$ ranged between 0.76 and 4.17 mm day$^{-1}$ for Calluancay and between 1.56 and 4.62 mm day$^{-1}$ for Cumbe. The difference can be attributed to the altitude difference between both catchments, with 900 m difference in elevation. The daily average minimum and maximum temperatures in Calluancay were 3.0 and 10.2 $^{o}$C respectively, while, in Cumbe they were 7.8 and 17.4 $^{o}$C. In addition, the wind speeds were different in both catchments. Calluancay is very exposed to prevailing winds while Cumbe is relatively sheltered. The daily average wind speeds for Calluancay and Cumbe were 4.2 (max: 11.9) and 0.9 (max: 2.6) m s$^{-1}$ respectively.

### 4.2 Modelling the discharge and the actual evapotranspiration

Table 3 and Fig. 4 summarize the results for the PDM model. The performance of the model for the calibration period is good in both catchments (Nash-Sutcliffe efficiency, NSE = 0.83). Lower values of NSE were obtained during the validation periods. The calibration focussed on low flows. More storm runoff events were observed during the validation period, as a consequence the poorer fit of large flows led to lower NSE.

The average soil moisture storage simulated by the PDM model was compared to the observed soil moisture measurements on representative plots (Fig. 4). Similar dynamics are observed. However, a more precise up-scaling (from plot to catchment) would benefit from more plots per catchment.

Table 2 shows the calibrated parameter set for both catchments. The maximum storage capacity $c_{max}$ is, as expected, higher at Calluancay. The parameter "b" is quite different between the 2 catchments. This difference of "b" can be partially attributed to the fact that Cumbe is much larger and less homogeneous and therefore, the variety of soils is larger which was reflected in the coefficient representing the variability of soil water storage capacity. The residence time for fast routing is very similar as expected with relatively small catchments. The residence time for slow routing is more different. We know according to recent research by Guzmán et al. (2016) that runoff from hillslopes in the Cumbe catchment infiltrates into the alluvial aquifer, which drains into the river and causes a slow reaction. Calluancay also showed somewhat more contribution of fast flow. This can be explained by the occurrence of saturated overland flow originating from the bogs and wetland parts of the páramo.

The daily average values of $E_a$, as estimated by the PDM model for Calluancay and Cumbe, were 1.47 (range 0.19 to 3.33) and 1.70 (range 0.18 to 3.58) mm day$^{-1}$ respectively. The PDM model, however, does not regard a critical soil moisture value for vegetation stress and therefore, there are no constraints on the evapotranspiration during dry periods. As a result, $E_a$ is overestimated by the model during these events.

The impact of both the vegetation and stress coefficients, globally represented by $K$ coefficient, was determined by means of a comparison between $E_a$ and $E_p$. For Calluancay and Cumbe, the impact of the aforementioned coefficient over the $E_a$ is on average 0.67 (range 0.09 to 1.00) and 0.58 (range 0.06 to 1.00) respectively. Buytaert et al. (2006c) determined two values of $K$ for natural and altered páramo vegetation during a period without soil water deficit ($k_s$ equals to 1), 0.42 and 0.58 respectively. The Calluancay value is similar. The $K$ value for Cumbe is in line with the literature for extensive grasslands (Allen et al., 1998).

Another important fact is that our soil water measurements never reached the wilting point; which is 0.43 and 0.30 cm$^3$ cm$^{-3}$ for Andosols (Calluancay) and Dystric Cambisols (Cumbe), respectively (Fig. 4 and Fig. S1 for the water retention curves in supplementary material). The minimum soil water content values during the drought periods in páramo and in Cumbe were not lower than 0.60 and 0.39 cm$^3$ cm$^{-3}$ respectively.

The average daily actual evapotranspiration rate of 1.47 and 1.70 mm day$^{-1}$ corresponds with former studies in páramo and grasslands respectively (Allen et al., 1998; Buytaert et al., 2006a). With the $E_a$ estimated, the $K$ coefficients were calculated in order to assess the combined effect of the vegetation and soil water stress. Values of 0.67 and 0.58 were obtained for páramo vegetation and grasslands respectively. The differences between the catchments are no more than a 16% comparing average values.

The relatively low values of $K$ could be partially explained by the plant physiology. The tussock grasses (mainly *Calamagrostis* spp. and *Stipa* spp.) in páramo are characterized by specific adaptations to extreme conditions. The plants have scleromorphic leaves which are essential to resist intense solar radiation (Ramsay and Oxley, 1997). In addition, the plants are surrounded by dead leaves that protect the plant and reduce the water uptake. In other words, the combination of the xerophytic properties and other adaptations to a high-radiation environment together with the dead leaves lead to a lower water demand as compared to the reference crop evapotranspiration. In Cumbe the grazing pastures are characterized by plants

of type C3 (*Pennisetum clandestinum*) which are also highly tolerant to drought. Therefore, the water uptake is mainly regulated by the plants during dry periods.

This can be clearly observed in the volumetric water content θ as measured by TDR (Fig. 4). Field observations in November 2009, revealed that the plants showed some visual signs of deterioration in the first centimetres but after removal of the top layer, which always contains dead leaves, the plants themselves showed little visual deterioration. Nevertheless, the depletion of the soil moisture storage during dry weather conditions clearly lead to stress and reduced the transpiration rate. As this vegetation has specific adaptations to high-radiation and cold environments, the recovery of the vegetation after drought is good. We also think that tillage, burning and artificial drainage might have a larger and more irreversible impact on the soil water holding capacity of the Andosol as compared to this "natural" drought.

### 4.3 The drought severity

Despite the fact that soil moisture measurements correspond to a plot-scale, they still give a good indication of the severity of the drought periods (Fig. 4). During the drought events in 2009 and 2010, the soil water content in the páramo dropped substantially, from a normal value of about 0.84 to ~ 0.60 $cm^3$ $cm^{-3}$. The soil moisture depletion observed in the mineral soils was similar to the Andosols (27%), decreasing from a normal value of about 0.54 to ~ 0.39 $cm^3$ $cm^{-3}$. Thus, it was possible to establish the amount of water of the topsoil which is available during these dry periods in páramo. The reservoir can deliver a water volume equivalent to 0.24 $cm^3$ $cm^{-3}$ (this represents the maximum soil water content change) during extreme climate conditions, such as the droughts in 2009 and 2010. In normal conditions the maximum change observed in the soil water content in páramo is no more than 0.05 $cm^3$ $cm^{-3}$.

In order to characterize the drought events at catchment scale, a standardized deficit as well as its duration were calculated for each catchment. The results are shown in Fig. 5. From this figure is clear to see that the deficit is no more than 9 days for both catchments. In other words, 9 days with mean flow are required to reduce the deficit to zero for the whole set of events. In addition, the duration of the drought events is relatively similar for both catchments with only few outliers as for the case of Cumbe.

This result was confirmed by the values of the slopes of the linear regression models (Fig. 5). One observes just a slightly higher value of the slope for the soil water storage in Calluancay (páramo) as compared to Cumbe (grassland). However, it is important to mention that the

values of the slopes reflect the effect of the drought propagation through the hydrological cycle. A reduced increase of deficit with duration was observed in both catchments. In addition, in Calluancay the standardized deficit and duration in soil water storage are highly correlated. In Cumbe, a high correlation was observed for the precipitation. To a lesser extent, a correlation was observed for the discharge for both catchments. The occurrence of hydrological drought events decreased due to high buffering capacity of the soils. This can explain the lack of a high correlation of the standardized deficit and duration in discharge, which has been widely documented in other studies (Van Loon et al., 2014; Peters et al., 2006).

### 4.4 The drought propagation

Fig. 6 shows the drought propagation plots for Calluancay and Cumbe. This figure confirms the results about the standardized deficit and duration for each drought event as well as the seasonality observed during the monitoring period. A series of quasi-consecutive drought periods was observed in the time series of precipitation during the dry season. The dry season normally occurs between August and November and the wet season is concentrated between February and June (Buytaert et al., 2006b; Celleri et al., 2007). Between August 2009 and March 2010 a drought period was observed; this event represented the longest episode with low rainfall for the whole time series. The soil water storage in both catchments had a crucial role in the propagation of the droughts. For instance, in Cumbe the meteorological drought event of 2009-2010 was almost completely buffered by the soil water storage and, hence, the hydrological drought was delayed. The opposite occurred in Calluancay, where the soil water storage at that time was not sufficient to overcome the period with low precipitation. The propagation of the drought was also observed simultaneously in the stream discharge (the hydrological drought). A different pattern is observed between 2010 and 2012. The buffering capacity of the soils in Calluancay was higher as compared to Cumbe, since a reduced number of hydrological drought events was observed during that period in Calluancay. The recovery of the soil water storage occurred during the wet season and was caused by several but intermittent storm events, which led to an irregular pattern of the soil water storage.

### 4.5 Soil water drought recovery

At the plot scale, the soil water content measured by TDR probes dropped from a normal value of about 0.84 to ~ 0.60 $cm^3$ $cm^{-3}$, while the recovery time was two to three months. This

did not occur at lower altitudes (Cumbe) where the mineral soils needed about eight months to recover from the drought in 2010. The soil moisture depletion observed in the mineral soils was from a normal value of about 0.54 to ~ 0.39 $cm^3$ $cm^{-3}$, but the recovery was slower (Fig. 4).

At the catchment scale, the following results were obtained with the PDM model. For the 2009-2010 drought event observed in Fig. 6, the duration of the soil water drought recovery for Calluancay and Cumbe was equal to 126 and 176 days respectively, while the meteorological drought durations were equal to 182 and 238 days respectively. The anomalies calculated were of -59% in Calluancay and -66% in Cumbe.

The soil water storage in both catchments decreased to about 3 mm at the beginning of the drought recovery. The speed of recovery expressed as percentage per day (which is the difference between the soil water storage at the end of drought and at the beginning of the drought recovery, divided by the time in days) was of 0.73 and 0.53 % recovery $day^{-1}$ for Calluancay and Cumbe respectively. This means that, the soil water recovery in Calluancay was a 37% faster as compared to Cumbe. The climate pattern observed for this event partially explains the differences between the rates of recovery. A higher evaporative demand was observed in Cumbe, as well as less rainfall. Over the duration of the recovery period, the difference of the precipitation in both catchments amounts to ca. 10%. The ratio between $P$ and $E_p$ in Calluancay is 50% higher for Calluancay than for Cumbe. For Calluancay and Cumbe, the soil water droughts started in August and July respectively. These months correspond to the dry season (July – November).

For the 2010-2011 soil water drought event, the drought recovery durations for Calluancay and Cumbe were 88 and 90 days respectively. The anomalies were of -61% (Calluancay) and -38% (Cumbe). The speed of recovery was relatively similar in both catchments despite the differences in the anomalies. The recovery rates were equal to 1.02 (Calluancay) and 0.94 % recovery $day^{-1}$ (Cumbe). This was almost identical. In this drought event, $E_p$ was significantly less than $P$, as compared with the first drought event. This meant more available water and less deficit. This fact and the difference in the anomalies can explain the similar recovery rate in both catchments for this event.

For the two major drought events the number of intermittent events were no more than 3. These events did not have a significant impact on the drought pattern.

On Fig. 6, we observed two small soil water drought events in 2011 in Calluancay and just one event in Cumbe. These dry periods occurred within the wet season and hence, the duration was no more than 50 days in both catchments (46 and 13 days for Calluancay and 34 days for Cumbe). The recovery rates for those events were equal to 3.03, 8.76 and 5.00 % recovery $day^{-1}$. The anomalies calculated for those events were different: -47.3% and -40.6% for Calluancay and -72.1% for Cumbe. The latest event was buffered almost completely by the soil water storage of Cumbe. This is confirmed by Fig. 6 where it is seen that a small hydrological drought event was generated by the anomaly observed in the precipitation. In a similar way, in Calluancay, the second event observed in that period was buffered by the soil water storage and, hence, a hydrological drought event was not generated.

In 2012, one minor soil water drought event was identified in Calluancay. The anomaly was equal to -44.7%. The drought recovery was reached in 8 days. The recovery rate was equal to 8.31% recovery $day^{-1}$. The duration of the drought was as short as 18 days.

### 4.6 The vegetation stress and recovery

Vegetation stress periods are identified as periods when the potential evapotranspiration exceeds the precipitation. Monthly data of $E_p$ and $P$ were used in the identification of the vegetation stress periods. For Calluancay the months from August 2009 to January 2010 clearly reveal a deficit of water (Fig. 7a). The modelling results confirmed that during this period $E_a$ was substantially reduced as compared to $E_p$. In addition, the end of the soil water drought happened in February 2010 (Fig. 6a), when the vegetation stress recovery started and the soil water content progressively increased during the wet season. The complete recovery was reached in June 2010 when $E_a$ was 92% of the $E_p$ (maximum value reached in the wet season).

Between August and November 2010, another vegetation stress period was identified. The vegetation stress recovery period was between December 2010 and April 2011 due to the onset of the wet season. The maximum monthly value of $E_a$ was equal to 86% of $E_p$ for this recovery period. While, the soil water drought recovery was reached in February 2011. In this month, $E_a$ was equal to 76% of $E_p$.

In 2011, August and October revealed a deficit of water with a quick recovery due to sufficient precipitation during November 2011 and February 2012 (here the maximum monthly $E_a$ was equal to 93% of $E_p$). While in 2012 the similar period between July and

September suffered a deficit. A partial recovery was observed in October and November 2012.

Finally, in Cumbe the vegetation stress was higher as compared to Calluancay (Fig.7b). From July 2009 to January 2010 seven consecutive months of vegetation stress took place in Cumbe. For instance, in August 2009 the total precipitation recorded in Cumbe was only 6.5 mm, while in Calluancay it was 24.2 mm. In February 2010, the end of the soil water drought recovery was observed and hence, this marked the beginning of the vegetation recovery period. The recovery was reached completely in June 2010 and as a consequence, $E_a$ was equal to 91% of $E_p$ (but with anomalies in March and April 2010) just before the onset of the second drought period.

The second vegetation stress period was identified between August 2010 and January 2011. Intermittent recoveries are observed during February and April 2011. In fact, these months were the end of the soil water drought recovery respectively. The $E_a$ estimated for those months was equal to 74 and 86% of $E_p$.

The third vegetation stress period was observed from August to December 2011. For this event, the recovery period was reached completely in February 2012 (only two months of recovery) and hence, the $E_a$ was equal to 86% of $E_p$. The last vegetation stress period was from March to November 2012. This marked the end of our monitoring period therefore we cannot provide an estimation of the complete recovery period.

### 4.7 Sensitivity analysis

Here, we studied two relatively simple scenarios, in both cases the parameter set obtained during the calibration procedure was kept. This means, the soil characteristics were not modified. Only precipitation and potential evapotranspiration were exchanged between the catchments in order to assess the impact on the soil water storage by means of simulations with the hydrological model. The sensitivity analysis was carried out over the period between May 2010 and November 2012 (Fig. 8). In this period, the difference of the precipitation in both catchments amounts to ca. 24%. The ratio between $P$ and $E_p$ in Calluancay was 61% higher for Calluancay than for Cumbe.

Fig. 8 revealed that the most important factor was the precipitation as compared to the potential evapotranspiration. The stream discharge was drastically reduced during the wet season in April 2012, as a consequence of the increase in the deficit of soil water storage. A

significant difference was not observed in the drought periods of 2009-2010 nor 2011 despite the increase in the rate of $E_p$ and by a reduction in the input of rain. The opposite occurred in Cumbe, mainly due to the increase in the precipitation amount and by a reduction in the potential evapotranspiration rate. Therefore, the stream discharge was substantially increased throughout the whole period, as a consequence of the reduction of soil water storage deficit. This illustrates the importance of whether the rainfall minus potential evapotranspiration shows a surplus or deficit.

### 4.8 Drought characteristics

The combinations of durations and standardized deficits for the drought events revealed no differences between the catchments. The maximum standardized deficit estimated was no more than nine days. This means that no more than nine days with mean flow are required to reduce the deficit to zero (Van Loon et al., 2014). While, the sensitivity analysis revealed that the precipitation is the main factor and has a direct influence over the hydrological response of the catchments, especially during the drought recovery.

The soil water drought propagation analysis showed the buffering capacity of the soil water storage. The buffering capacity of the soils was important in the drought of 2010-2011 and partially in the previous event of 2009-2010. Comparing the drought analysis for soil water storage and stream discharge clearly showed that they were linked. The seasonality observed in the rainfall climate during the monitoring period is also reflected by the temporal variability of the soil water storage with some delay due to buffering.

In the drought event of 2009-2010, the vegetation stress observed in Cumbe seven consecutive months of water deficit were recorded as compared to six months in Calluancay. The onset of the drought coincided with the dry season. The vegetation recovery occurred during the wet season in both catchments and when the maximum actual evapotranspiration reached 93% of the potential vegetation evapotranspiration.

After the drought event of 2009-2010 in Calluancay and Cumbe, the vegetation recovery was reached in three and five months, respectively. For Calluancay, the three months were consecutive, while in Cumbe the recovery occurred with intermittent periods of stress. In the second drought event of 2010-2011, the recovery was equal to five and six months for Calluancay and Cumbe respectively.

Finally, point measurements of soil water content in both catchments revealed high differences during drought events (Fig. 4). A faster recovery was observed in páramo as compared to the grasslands of Cumbe. Nevertheless, whether soil water storage simulations - catchment scale- are used instead of plot measurements, the differences in the speed of recovery is no more than 37% (drought event 2009-2010).

## 5 Conclusions

The páramo ecosystem has a pivotal role in the hydrology and ecology of the highlands above 3500m in the Andean region and it is a major source of water for human consumption, irrigation and hydropower. Therefore, we compared the hydrological response of a typical catchment on the páramo at 3500 m a.s.l. to one with a lower grassland at 2600 m a.s.l. during drought events in 2009, 2010, 2011 and 2012. The analysis was carried out based on the calibration and validation of a hydrological conceptual model, the PDM model and compared to soil water measurements in plots.

Based on the threshold method, the soil moisture droughts occurred mainly in the dry season in both catchments as a consequence of several anomalies in the precipitation (meteorological drought). Just one soil moisture drought was observed during the wet season (in 2011). The deficit for all cases was small and progressively reduced during the wet season. This conclusion was confirmed by the identification of the vegetation stress periods. These periods correspond mainly to the months of September, October and November which coincided with the dry season. In this context, the maximum number of consecutive dry days was reached during the droughts of 2009 and 2010, i.e. 19 and 22 days, which can be considered a very long period in the páramo. In these periods, the soil moisture content observed in the experimental plot reached also the lowest values recorded until now, 0.60 $cm^3$ $cm^{-3}$ in November 2009.

At the plot scale the differences between the recovery of the soils were relatively large. The measured water content in páramo soils showed a quicker recovery as compared to the mineral soils in Cumbe. At the catchment scale, however, the soil water storage simulated by the PDM model and the drought analysis was not as pronounced. Only for the prolonged drought event of 2009-2010 the differences were larger.

At high altitudes, the lower temperatures and the lower water demand for vegetation lead to lower values of the evapotranspiration. The difference between the rainfall and the potential evapotranspiration has been shown to have more impact on the regional difference in hydrologic behaviour than the difference between the water storage capacities of the soils. In the experimental catchments we monitored, the soils never became extremely dry nor close to wilting point. This may explain the fact that the soil water storage capacity had only a secondary influence as it was never fully depleted.

## Acknowledgements

We thank the VLIR-IUC programme and IFS for its financial support during this research project. Thanks also to the editor, the anonymous referee and Dr. Wouter Buytaert for their comments in order to improve the present manuscript.

## References

Allen, R., Pereira, L. S., Raes, D. and Smith, M.: Crop evapotranspiration. Guidelines for Computing Crop Water Requirements. FAO Irrigation and Drainage Paper 56. FAO, Rome., 1998.

Andreadis, K. M., Clark, E. a., Wood, A. W., Hamlet, A. F. and Lettenmaier, D. P.: Twentieth-Century Drought in the Conterminous United States, Journal of Hydrometeorology, 6(6), 985–1001, doi:10.1175/JHM450.1, 2005.

Buytaert, W. and Beven, K.: Models as multiple working hypotheses: hydrological simulation of tropical alpine wetlands, Hydrological Processes, 25(11), 1784–1799, doi:10.1002/hyp.7936, 2011.

Buytaert, W. and De Bièvre, B.: Water for cities: The impact of climate change and demographic growth in the tropical Andes, Water Resources Research, 48(8), W08503, doi:10.1029/2011WR011755, 2012.

Buytaert, W., Célleri, R., De Bièvre, B., Cisneros, F., Wyseure, G., Deckers, J. and Hofstede, R.: Human impact on the hydrology of the Andean páramos, Earth-Science Reviews, 79(1-2), 53–72, doi:10.1016/j.earscirev.2006.06.002, 2006a.

Buytaert, W., Celleri, R., Willems, P., Bièvre, B. De and Wyseure, G.: Spatial and temporal rainfall variability in mountainous areas: A case study from the south Ecuadorian Andes, Journal of Hydrology, 329(3-4), 413–421, doi:10.1016/j.jhydrol.2006.02.031, 2006b.

Buytaert, W., Cuesta-Camacho, F. and Tobón, C.: Potential impacts of climate change on the environmental services of humid tropical alpine regions, Global Ecology and Biogeography, 20(1), 19–33, doi:10.1111/j.1466-8238.2010.00585.x, 2011.

Buytaert, W., Deckers, J. and Wyseure, G.: Regional variability of volcanic ash soils in south

Ecuador: The relation with parent material, climate and land use, Catena, 70(2), 143–154, doi:10.1016/j.catena.2006.08.003, 2007a.

Buytaert, W., Iñiguez, V. and Bièvre, B. De: The effects of afforestation and cultivation on water yield in the Andean páramo, Forest Ecology and Management, 251(1-2), 22–30, doi:10.1016/j.foreco.2007.06.035, 2007b.

Buytaert, W., Iñiguez, V., Celleri, R., De Bièvre, B., Wyseure, G. and Deckers, J.: Analysis of the Water Balance of Small Páramo Catchments in South Ecuador, in Environmental Role of Wetlands in Headwaters SE - 24, vol. 63, edited by J. Krecek and M. Haigh, pp. 271–281, Springer Netherlands, Dordrecht, The Netherlands., 2006c.

Buytaert, W., Vuille, M., Dewulf, A., Urrutia, R., Karmalkar, A. and Célleri, R.: Uncertainties in climate change projections and regional downscaling in the tropical Andes: implications for water resources management, Hydrology and Earth System Sciences, 14(7), 1247–1258, doi:10.5194/hess-14-1247-2010, 2010.

Buytaert, W., Wyseure, G., De Bièvre, B. and Deckers, J.: The effect of land-use changes on the hydrological behaviour of Histic Andosols in south Ecuador, Hydrological Processes, 19(20), 3985–3997, doi:10.1002/hyp.5867, 2005.

Celleri, R., Willems, P., Buytaert, W. and Feyen, J.: Space–time rainfall variability in the Paute basin, Ecuadorian Andes, Hydrological Processes, 21(24), 3316–3327, doi:10.1002/hyp.6575, 2007.

Dai, A.: Drought under global warming: A review, Wiley Interdisciplinary Reviews: Climate Change, 2(1), 45–65, doi:10.1002/wcc.81, 2011.

Dercon, G., Bossuyt, B., De Bièvre, B., Cisneros, F. and Deckers, J.: Zonificación agroecológica del Austro Ecuatoriano, U Ediciones, Cuenca, Ecuador., 1998.

Dercon, G., Govers, G., Poesen, J., Sánchez, H., Rombaut, K., Vandenbroeck, E., Loaiza, G. and Deckers, J.: Animal-powered tillage erosion assessment in the southern Andes region of Ecuador, Geomorphology, 87(1-2), 4–15, doi:10.1016/j.geomorph.2006.06.045, 2007.

Duan, Q., Sorooshian, S. and Gupta, V.: Effective and efficient global optimization for conceptual rainfall-runoff models, Water Resources Research, 28(4), 1015–1031, doi:10.1029/91WR02985, 1992.

FAO, ISRIC and ISSS: World Reference Base for Soil Resources. No. 84 in World Soil Resources Reports. FAO, Rome., 1998.

Farley, K. a., Kelly, E. F. and Hofstede, R. G. M.: Soil Organic Carbon and Water Retention after Conversion of Grasslands to Pine Plantations in the Ecuadorian Andes, Ecosystems, 7(7), 729–739, doi:10.1007/s10021-004-0047-5, 2004.

Garcia, M., Raes, D., Allen, R. and Herbas, C.: Dynamics of reference evapotranspiration in the Bolivian highlands (Altiplano), Agricultural and Forest Meteorology, 125(1-2), 67–82, doi:10.1016/j.agrformet.2004.03.005, 2004.

Guzmán, P., Anibas, C., Batelaan, O., Huysmans, M. and Wyseure, G.: Hydrological connectivity of alluvial Andean valleys: a groundwater/surface-water interaction case study in Ecuador, Hydrogeology Journal, doi:10.1007/s10040-015-1361-z, 2016.

Hargreaves, G. H. and Samani, Z. A.: Reference Crop Evapotranspiration from Temperature, Applied Engineering in Agriculture, 1(2), 96–99, 1985.

Hofstede, R. G. M., Groenendijk, J. P., Coppus, R., Fehse, J. C. and Sevink, J.: Impact of Pine Plantations on Soils and Vegetation in the Ecuadorian High Andes, Mountain Research and Development, 22(2), 159–167, doi:10.1659/0276-4741(2002)022[0159:IOPPOS]2.0.CO;2, 2002.

Hofstede, R., Segarra, P. and Mena, P.: Los páramos del mundo, Global Peatland Initiative/NC-IUCN/EcoCiencia, Quito., 2003.

Hungerbühler, D., Steinmann, M., Winkler, W., Seward, D., Egüez, A., Peterson, D. E., Helg, U. and Hammer, C.: Neogene stratigraphy and Andean geodynamics of southern Ecuador, Earth-Science Reviews, 57(1-2), 75–124, doi:10.1016/S0012-8252(01)00071-X, 2002.

Kilpatrick, F. and Schneider, V.: Use of flumes in measuring discharge, U.S. Geological Survey Techniques of Water Resources Investigations, Washington, USA., 1983.

Klemeš, V.: Operational testing of hydrological simulation models, Hydrological Sciences Journal, 31(1), 13–24, doi:10.1080/02626668609491024, 1986.

Koch, K., Wenninger, J., Uhlenbrook, S. and Bonell, M.: Joint interpretation of hydrological and geophysical data: electrical resistivity tomography results from a process hydrological research site in the Black Forest Mountains, Germany, Hydrological Processes, 23(10), 1501–1513, doi:10.1002/hyp.7275, 2009.

Liefvendahl, M. and Stocki, R.: A study on algorithms for optimization of Latin hypercubes, Journal of Statistical Planning and Inference, 136(9), 3231–3247, doi:10.1016/j.jspi.2005.01.007, 2006.

Lloyd-Hughes, B. and Saunders, M. A.: A drought climatology for Europe, International Journal of Climatology, 22(13), 1571–1592, doi:10.1002/joc.846, 2002.

Luteyn, J. L.: Páramos: A Checklist of Plant Diversity, Geographical Distribution, and Botanical Literature. The New York Botanical Garden Press, New York., 1999.

Moore, R. J.: The probability-distributed principle and runoff production at point and basin scales, Hydrological Sciences Journal, 30(2), 273–297, doi:10.1080/02626668509490989, 1985.

Moore, R. J. and Clarke, R. T.: A distribution function approach to rainfall runoff modeling, Water Resources Research, 17(5), 1367–1382, doi:10.1029/WR017i005p01367, 1981.

Mora, D. E., Campozano, L., Cisneros, F., Wyseure, G. and Willems, P.: Climate changes of hydrometeorological and hydrological extremes in the Paute basin, Ecuadorean Andes, Hydrology and Earth System Sciences, 18(2), 631–648, doi:10.5194/hess-18-631-2014, 2014.

Nash, J. E. and Sutcliffe, J. V.: River flow forecasting through conceptual models part I — A discussion of principles, Journal of Hydrology, 10(3), 282–290, doi:10.1016/0022-1694(70)90255-6, 1970.

Parry, S., Wilby, R. L., Prudhomme, C. and Wood, P. J.: A systematic assessment of drought termination in the United Kingdom, Hydrology and Earth System Sciences Discussions, (January), 1–33, doi:10.5194/hess-2015-476, 2016.

Pebesma, E. J.: Multivariable geostatistics in S: the gstat package, Computers & Geosciences, 30(7), 683–691, doi:10.1016/j.cageo.2004.03.012, 2004.

Peters, E., Bier, G., van Lanen, H. A. J. and Torfs, P. J. J. F.: Propagation and spatial distribution of drought in a groundwater catchment, Journal of Hydrology, 321(1-4), 257–

275, doi:10.1016/j.jhydrol.2005.08.004, 2006.

Podwojewski, P., Poulenard, J., Zambrana, T. and Hofstede, R.: Overgrazing effects on vegetation cover and properties of volcanic ash soil in the páramo of Llangahua and La Esperanza (Tungurahua, Ecuador), Soil Use and Management, 18, 45–55, doi:10.1111/j.1475-2743.2002.tb00049.x, 2002.

Ramsay, P. M. and Oxley, E. R. B.: The growth form composition of plant communities in the ecuadorian páramos, Plant Ecology, 131(2), 173–192, doi:10.1023/A:1009796224479, 1997.

Romano, N.: Soil moisture at local scale: Measurements and simulations, Journal of Hydrology, 516, 6–20, doi:10.1016/j.jhydrol.2014.01.026, 2014.

Schneider, P., Vogt, T., Schirmer, M., Doetsch, J., Linde, N., Pasquale, N., Perona, P. and Cirpka, O. a.: Towards improved instrumentation for assessing river-groundwater interactions in a restored river corridor, Hydrology and Earth System Sciences, 15(8), 2531–2549, doi:10.5194/hess-15-2531-2011, 2011.

Southgate, D. and Macke, R.: The Downstream Benefits of Soil Conservation in Third World Hydroelectric Watersheds, Land Economics, 65(1), 38, doi:10.2307/3146262, 1989.

Stocki, R.: A method to improve design reliability using optimal Latin hypercube sampling, Computer Assisted Mechanics and Engineering Sciences, (12), 393–411, 2005.

Tsakiris, G., Nalbantis, I., Vangelis, H., Verbeiren, B., Huysmans, M., Tychon, B., Jacquemin, I., Canters, F., Vanderhaegen, S., Engelen, G., Poelmans, L., De Becker, P. and Batelaan, O.: A System-based Paradigm of Drought Analysis for Operational Management, Water Resources Management, 27(15), 5281–5297, doi:10.1007/s11269-013-0471-4, 2013.

Vanacker, V., Molina, A., Govers, G., Poesen, J. and Deckers, J.: Spatial variation of suspended sediment concentrations in a tropical Andean river system: The Paute River, southern Ecuador, Geomorphology, 87(1-2), 53–67, doi:10.1016/j.geomorph.2006.06.042, 2007.

van Genuchten, M. T.: A Closed-form Equation for Predicting the Hydraulic Conductivity of Unsaturated Soils, Soil Science Society of America Journal, 44, 892–898, doi:10.2136/sssaj1980.03615995004400050002x, 1980.

Van Lanen, H. A. J., Wanders, N., Tallaksen, L. M. and Van Loon, A. F.: Hydrological drought across the world: impact of climate and physical catchment structure, Hydrology and Earth System Sciences, 17(5), 1715–1732, doi:10.5194/hess-17-1715-2013, 2013.

Van Loon, a. F., Tijdeman, E., Wanders, N., Van Lanen, H. A. J., Teuling, a. J. and Uijlenhoet, R.: How climate seasonality modifies drought duration and deficit, Journal of Geophysical Research: Atmospheres, 119(8), 4640–4656, doi:10.1002/2013JD020383, 2014.

Van Loon, A. F.: On the propagation of drought. How climate and catchment characteristics influence hydrological drought development and recovery, PhD Thesis, Wageningen University, Wageningen, the Netherlands., 2013.

Van Loon, A. F.: Hydrological drought explained, Wiley Interdisciplinary Reviews: Water, 2(4), 359–392, doi:10.1002/wat2.1085, 2015.

Vicente-Serrano, S. M., Gouveia, C., Camarero, J. J., Beguería, S., Trigo, R., López-Moreno, J. I., Azorín-Molina, C., Pasho, E., Lorenzo-Lacruz, J., Revuelto, J., Morán-Tejeda, E. and

Sanchez-Lorenzo, A.: Response of vegetation to drought time-scales across global land biomes., Proceedings of the National Academy of Sciences of the United States of America, 110(1), 52–7, doi:10.1073/pnas.1207068110, 2013.

Viviroli, D., Archer, D. R., Buytaert, W., Fowler, H. J., Greenwood, G. B., Hamlet, a. F., Huang, Y., Koboltschnig, G., Litaor, M. I., López-Moreno, J. I., Lorentz, S., Schädler, B., Schreier, H., Schwaiger, K., Vuille, M. and Woods, R.: Climate change and mountain water resources: overview and recommendations for research, management and policy, Hydrology and Earth System Sciences, 15(2), 471–504, doi:10.5194/hess-15-471-2011, 2011.

Wagener, T., Boyle, D. P., Lees, M. J., Wheater, H. S., Gupta, H. V. and Sorooshian, S.: A framework for development and application of hydrological models, Hydrology and Earth System Sciences, 5(1), 13–26, doi:10.5194/hess-5-13-2001, 2001.

**Table 1.** The main characteristics of the experimental catchments

| Name | Calluancay | Cumbe |
|---|---|---|
| Area [$km^2$] | 4.39 | 44.0 |
| Altitude [m a.s.l.] | 3589 - 3882 | 2647 - 3467 |
| Observation period | Nov 2007 – Nov 2012 | Apr 2009 – Nov 2012 |
| **Hydrometeorological variables:** | | |
| $P$ [mm $year^{-1}$] | 1095 | 783 |
| $E_p$ [mm $year^{-1}$] | 831 | 1100 |
| $Q$ [mm $year^{-1}$] | 619 | 181 |
| **-State variables:** | | |
| Soil water content [$cm^3$ $cm^{-3}$][a] | 0.60 – 0.86 | 0.39 – 0.54 |

[a], The average daily minimum and maximum soil water contents for each observation period

**Table 2.** The calibrated parameters of the PDM model.

| Parameters | Description | Feasible range | Calluancay | Cumbe |
|---|---|---|---|---|
| $c_{max}$ | Maximum storage capacity | 30-75 [mm] | 64.8 | 54.5 |
| $b$ | Spatial variability of the storage capacity | 0.1-2.0 [-] | 0.74 | 0.17 |
| $f_{rt}$ | Fast routing store residence time | 1-2 [days] | 1.5 | 1.4 |
| $s_{rt}$ | Slow routing store residence time | 35-120 [days] | 58.3 | 98.2 |
| %($q$) | Percentage of fast flow | 0.25-0.75 [-] | 0.51 | 0.41 |

**Table 3.** The Nash and Sutcliffe efficiencies for the PDM models*.

| | Calibration | | Validation | |
|---|---|---|---|---|
| Catchment | NS (-) | Period | NS (-) | Period |
| Calluancay | 0.83 | 29 Nov 2007 – 06 Ago 2009 | 0.53 | 20 May 2010 – 27 Nov 2012 |
| Cumbe | 0.84 | 21 Apr 2009 – 17 Apr 2011 | 0.63 | 18 Apr 2011 – 13 Dec 2012 |

*NS is the Nash and Sutcliffe efficiency based on the logarithms of stream discharges

**Figure 1.** The study area

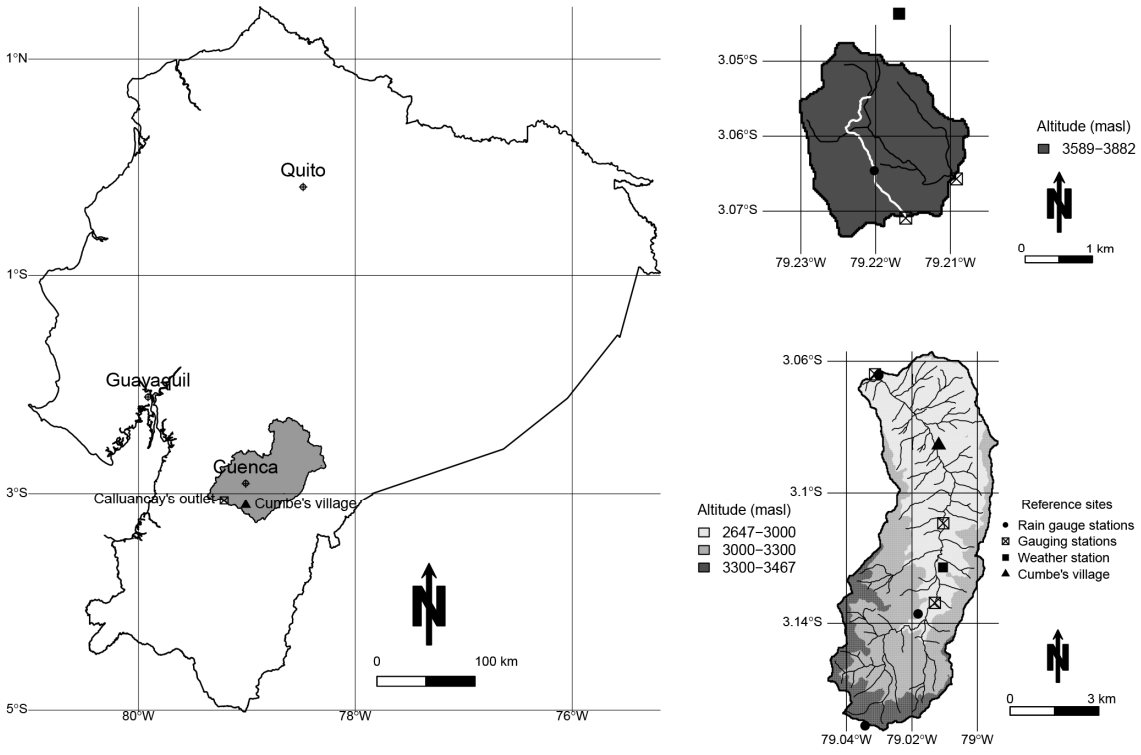


**Figure 2.** Conceptual diagram for the estimation of the soil moisture drought recovery metrics. $t_d$ and $t_{dr}$ are the durations of the soil moisture drought event and drought recovery period respectively. The drought recovery is represented by a brown line. The grey arrows mark intermittent events above the threshold. The green line marks the assumed normal value of the soil water storage.

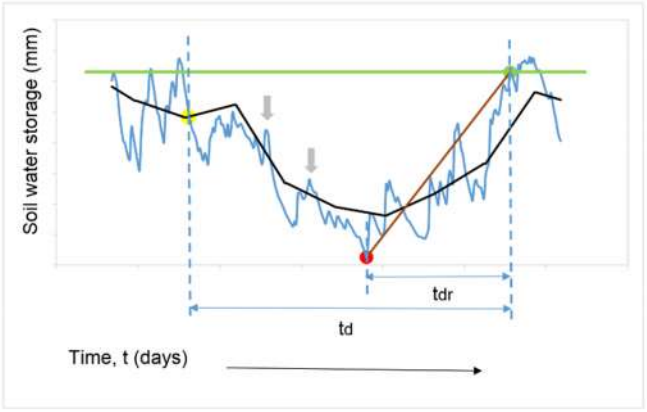

**Figure 3.** The potential evapotranspiration $E_p$ for Calluancay (black) and Cumbe (grey).

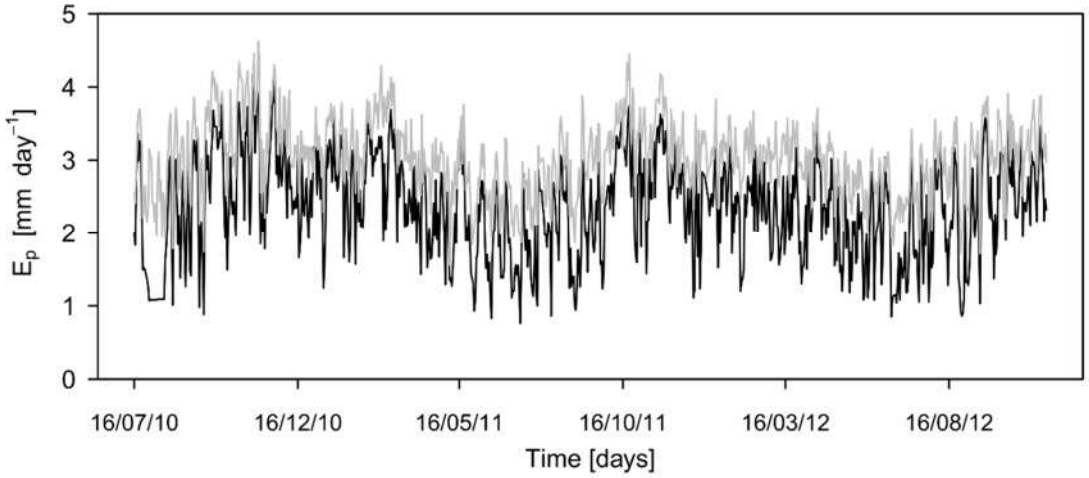


**Figure 4.** Results from the hydrological modelling with the PDM model.

Panel 1: precipitation; Panel 2: observed ($Q_{obs}$) and simulated ($Q_{sim}$) river discharge; Panel 3: simulated average soil water storage; Panel 4: soil moisture measured in an experimental plot.

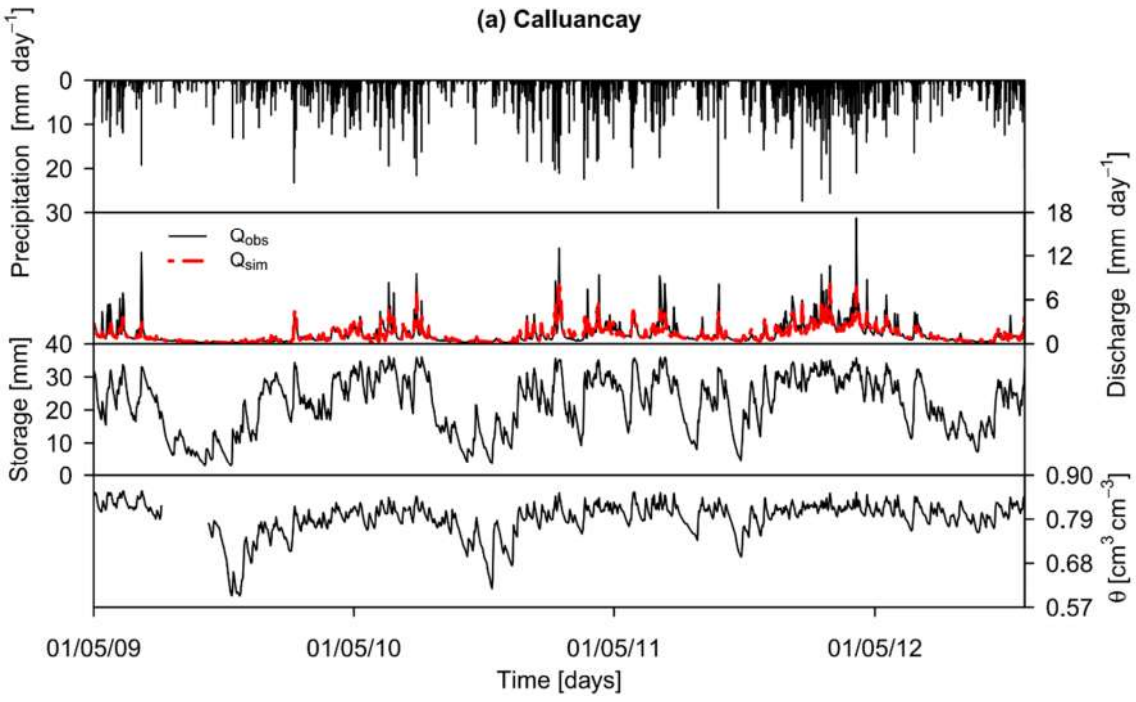

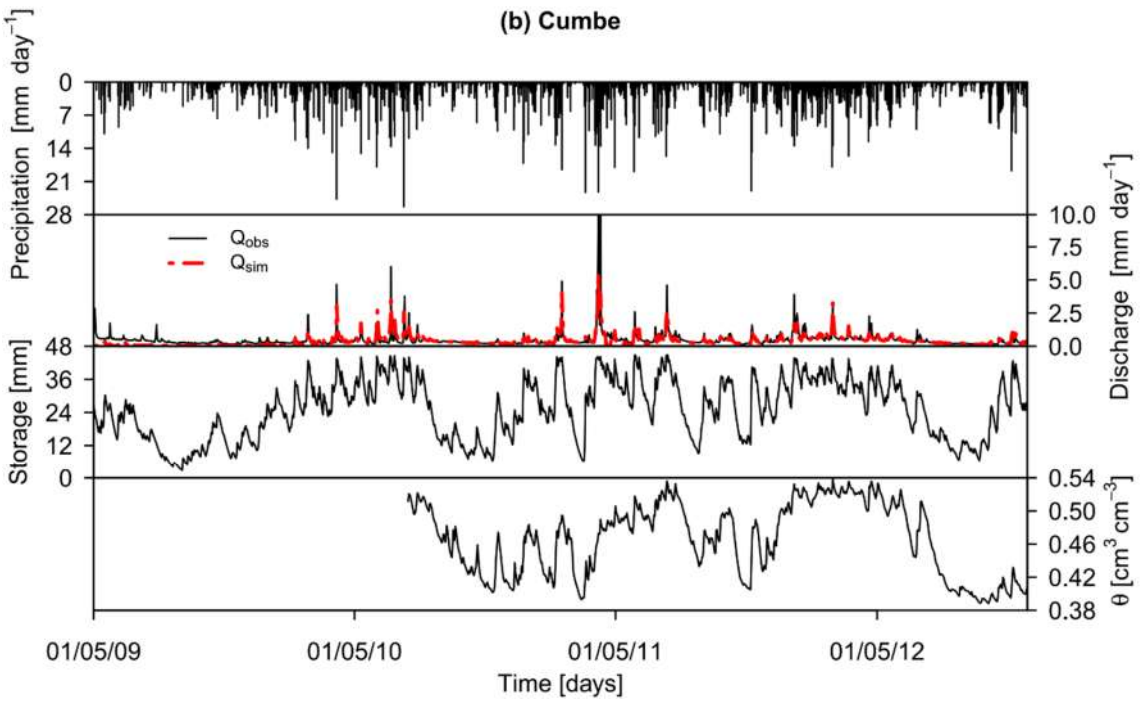


**Figure 5.** Standardized deficit for the drought periods in (a) Calluancay and (b) Cumbe: Precipitation (*P*, in blue); simulated soil water storage (*S*, in black) and observed stream discharge (*Q*, in red).

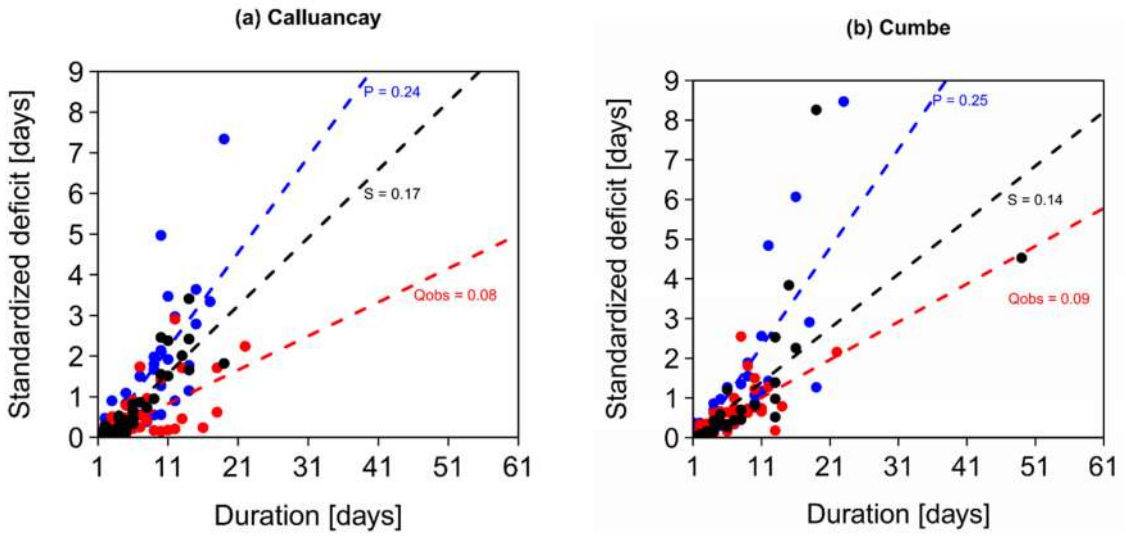

**Figure 6.** Drought propagation for each experimental catchment. The discharge corresponds to the observed data. The soil water storage is the storage simulated by the PDM model.

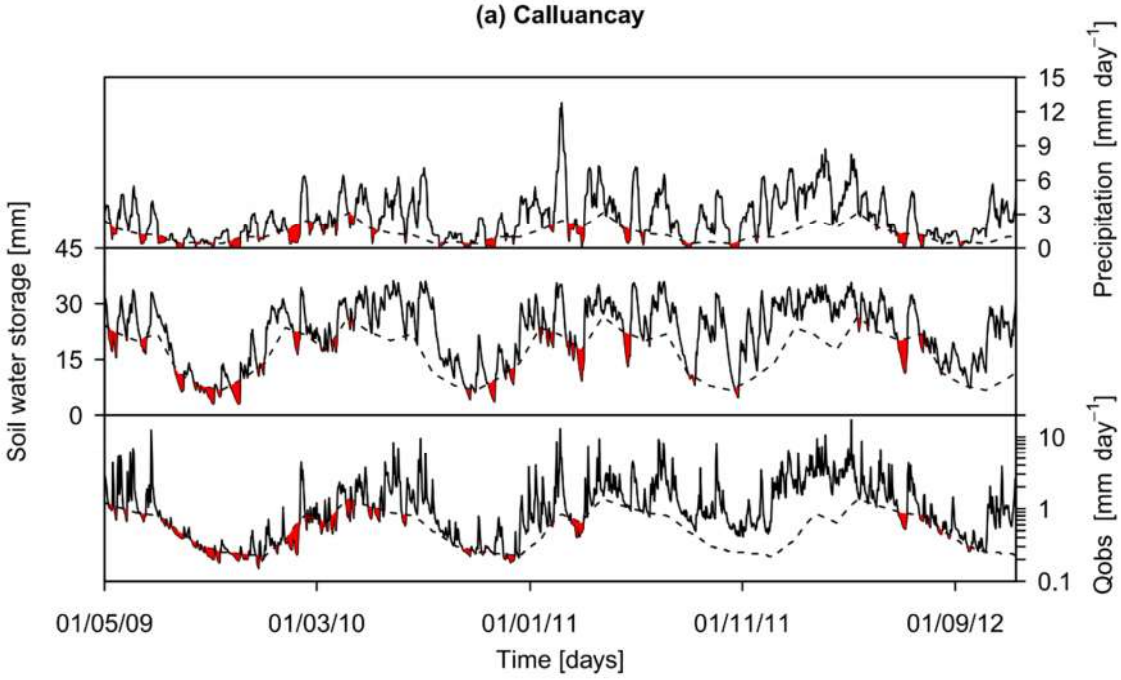


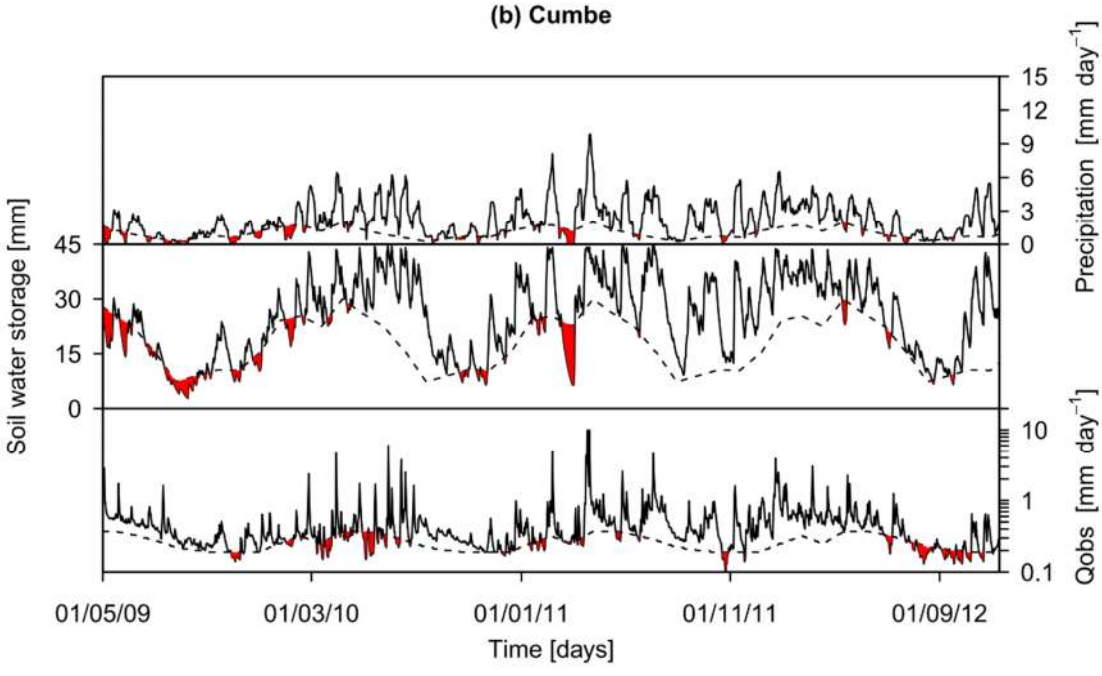

**Figure 7**. Time series of precipitation ($P$), potential evapotranspiration ($E_p$) and actual evapotranspiration ($E_a$) in order to identify vegetation stress and recovery periods

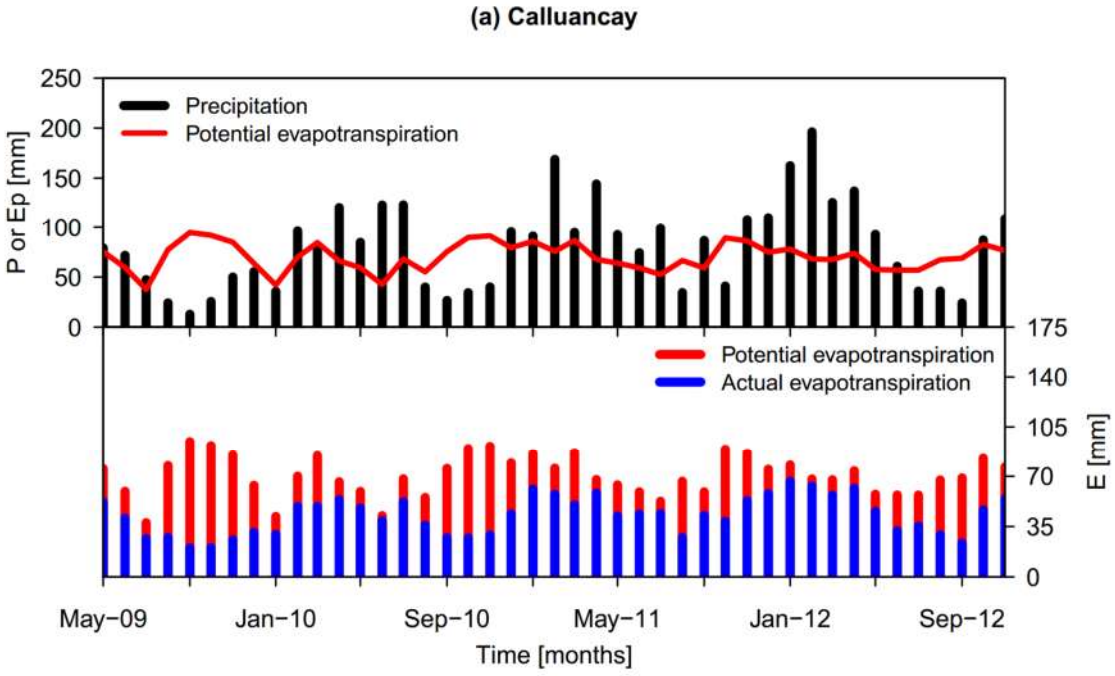


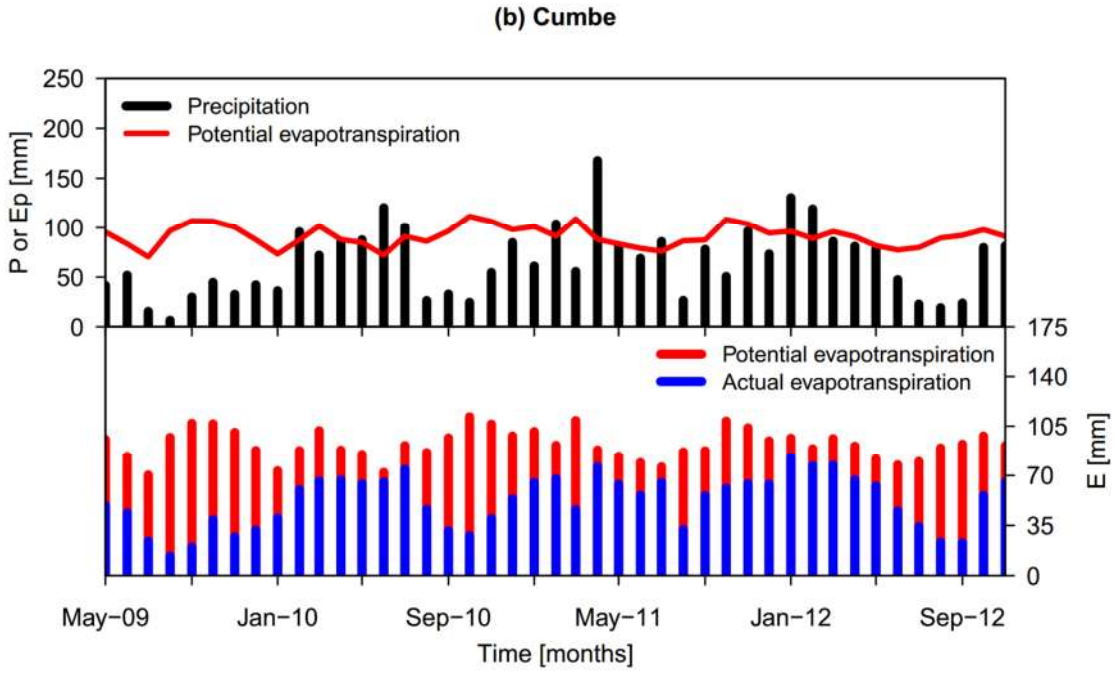

**Figure 8.** Soil water storage and stream discharge for the experimental catchments as result of the two climate scenarios. The simulated time series for the storage and the stream discharge are included for comparison.